ARTICLES

Kinetic Study and Determination of the Enthalpies of Activation of the Dehydrogenation of Titanium- and Zirconium-Doped $NaAlH_4$ and Na_3AlH_6

Tetsu Kiyobayashi,[†] Sesha S. Srinivasan,[‡] Dalin Sun,[‡] and Craig M. Jensen*[,‡]

National Institute of Advanced Science and Technology, Midorigaoka 1-8-31, Ikeda, Osaka 563-8577, Japan, and Department of Chemistry, University of Hawaii, Honolulu, Hawaii 96822

Received: March 3, 2003; In Final Form: July 2, 2003

The rates of the dehydrogenation of the sodium alanates $NaAlH_4$ and Na_3AlH_6 doped with 2 mol % Ti or Zr have been measured over the temperature range 363−423 K. $NaAlH_4$ and Na_3AlH_6 undergo dehydrogenation at equal rates upon direct doping with titanium. However, Na_3AlH_6 arising from the dehydrogenation of Ti-doped $NaAlH_4$ undergoes dehydrogenation at much slower rates. Rate constants were determined from the slopes of the dehydrogenation profiles. On the basis of Eyring theory, the enthalpies of activation, $\Delta H^{\ddagger}$, for the dehydrogenation reactions were determined to be ∼100 kJ·mol^{-1} for both Ti-doped $NaAlH_4$ and Na_3AlH_6 and ∼135 kJ·mol^{-1} for both Zr-doped $NaAlH_4$ and Na_3AlH_6. These results suggest that the dehydrogenation reaction pathways are highly sensitive to the nature and distribution of the dopant but not to differences in the Al−H bonding interactions in $[AlH_4]^-$ and $[AlH_6]^{3-}$ complex anions. Furthermore, we conclude that the kinetics are probably influenced by processes such as nucleation and growth and/or range atomic transport phenomenon.

Introduction

The development of high-performance hydrogen carriers is becoming increasingly important with the approach of practical, hydrogen-powered vehicles and electronic devices. Over the past several decades, metal hydrides have been utilized in limited applications as hydrogen storage materials. However, a "holy grail" material having both a high hydrogen capacity (≥5 wt % available hydrogen)[1] and rapid hydrogen cycling kinetics at low temperatures has not been attained despite the considerable research efforts that have been concentrated on MgH_2 and a variety of interstitial hydrides.[2] A number of complex hydrides have considerably high hydrogen capacities. However, until recently, they were precluded from consideration as potential hydrogen storage materials due to their slow dehydrogenation kinetics and poor reversibility. This thinking was changed by the finding that charging $NaAlH_4$ with a few mole percent of selected transition metal dopants significantly enhances the kinetics of the dehydrogenation process and renders it reversible in the solid state under moderate conditions.[3,4] This breakthrough has been followed by a great deal of effort to develop alanates as practical hydrogen storage materials.[5−23] However, the mechanism by which the dopants enhance the dehydrogenation of $NaAlH_4$ remains an enigma. An understanding of the mechanistic role of the dopants would aid the development of alanates that are suitable for practical applications.

The present study was conducted to obtain quantitative information about the effect of titanium and zirconium dopants on the dehydrogenation of $NaAlH_4$ and Na_3AlH_6. We have carried out systematic kinetic measurements over the temperature range 363−423 K and interpreted the resulting dehydrogenation profiles. This information has provided us with insights into the dehydrogenation mechanisms of $NaAlH_4$ and Na_3AlH_6.

Experimental Section

Materials. Titanium *n*-butoxide, $Ti(OBu^n)_4$, and zirconium *n*-propoxide, $Zr(OPr^n)_4$, were obtained from Aldrich Chemical Inc. and used as received. Sodium aluminum hydride, $NaAlH_4$, was obtained from Albemarle Corp. and recrystallized from tetrahydrofuran prior to use. $NaAlH_4$ was doped with 2 mol % $Ti(OBu^n)_4$ of $Zr(OPr^n)_4$ according to the published procedure.[5,14]

Kinetic Measurements. The dehydrogenation studies were carried out using an automated Sieverts' type apparatus (LESCA Co), which allowed for the accurate volumetric determination of the amounts of hydrogen evolved. Rapid heating of the sample to the desired temperature was accomplished by immersing the sample reactor into a silicon oil bath (accuracy of ±1 K) preheated to a given temperature. Dehydrogenation was performed against a back pressure of 0.1 MPa in a fixed volume.

Theory of Data Analysis. The dehydrogenation of $NaAlH_4$ is composed of a two-step process seen in eqs 1 and 2.

$$NaAlH_4 \xrightarrow{k_1} \frac{1}{3}Na_3AlH_6 + \frac{2}{3}Al + H_2 \quad (1)$$

$$Na_3AlH_6 \xrightarrow{k_2} 3NaH + Al + \frac{3}{2}H_2 \quad (2)$$

Assuming these reactions to be first-order and independent, the differential form of the rate equation is

* Corresponding author. Phone: 1-808-956-2769. Fax: 1-808-956-5908. E-mail: jensen@gold.chem.hawaii.edu.
[†] National Institute of Advanced Science and Technology.
[‡] University of Hawaii.

10.1021/jp034543h CCC: $25.00
Published on Web 09/03/2003

$$\frac{dN_A(t)}{dt} = -k_i N_A(t) \qquad (A = NaAlH_4, Na_3AlH_6; i = 1, 2) \tag{3}$$

The solution of eq 3 gives

$$-k_i t = \ln\left(\frac{N_A(t)}{N_A{}^0}\right) \tag{4}$$

where k_i is the reaction rate constant and $N_A(t)$ and $N_A{}^0$ are the moles of the substance A present at times t and $t = 0$, respectively. It is appropriate to substitute $N_{H_2}(t)$ for $N_A(t)$ in eq 4 because moles of hydrogen, $N_{H_2}(t)$, rather than $N_A(t)$ were directly determined in our experiments. In terms of the stoichiometric factors of reactions in eqs 1 and 2, we obtain the relations between $N_{H_2}(t)$ and the rate constant k_i as

$$-k_1 t = \ln\left(1 - \frac{N_{H_2}(t)}{N_{NaAlH_4}{}^0}\right) \tag{5}$$

for the dehydrogenation of $NaAlH_4$ and

$$-k_2 t = \ln\left(1 - \frac{2N_{H_2}(t)}{3N_{Na_3AlH_6}{}^0}\right) \tag{6}$$

for that of Na_3AlH_6.

When the reactions in eqs 1 and 2 are treated as consecutive first-order reactions, the simultaneous differential equations

$$\frac{dN_{NaAlH_4}(t)}{dt} = -k_1 N_{NaAlH_4}$$

$$\frac{dN_{Na_3AlH_6}(t)}{dt} = -k_2 N_{Na_3AlH_6} + \frac{1}{3}k_1 N_{NaAlH_4} \tag{7}$$

yield the solution

$$\frac{N_{NaAlH_4}(t)}{N_{NaAlH_4}{}^0} = \exp(-k_1 t) \tag{8}$$

and

$$\frac{N_{Na_3AlH_6}(t)}{N_{NaAlH_4}{}^0} = \frac{1}{3}\frac{k_1}{k_1 - k_2}\{\exp(-k_2 t) - \exp(-k_1 t)\} \tag{9}$$

by applying the initial condition $N_{Na_3AlH_6}{}^0 = 0$. For the same reason as mentioned above, $N_{H_2}(t)$ is substituted for $N_{NaAlH_4}(t)$ and $N_{Na_3AlH_6}(t)$ in eqs 8 and 9. Thus the relation between $N_{H_2}(t)$ and the rate constants k_1 and k_2 is obtained,

$$\frac{N_{H_2}(t)}{N_{NaAlH_4}{}^0} = \left\{1 - \frac{k_2}{2(k_1 - k_2)}\right\}\{1 - \exp(-k_1 t)\} + \left\{\frac{k_1}{2(k_1 - k_2)}\right\}\{1 - \exp(-k_2 t)\} \tag{10}$$

The first term on the right-hand side of eq 10 is the contribution from the dehydrogenation of $NaAlH_4$, and the second term is that of Na_3AlH_6.

According to the Eyring theory,[24] the relation between the rate constant k_i and the Gibbs free energy of activation $\Delta G^{\ddagger}$ is given by

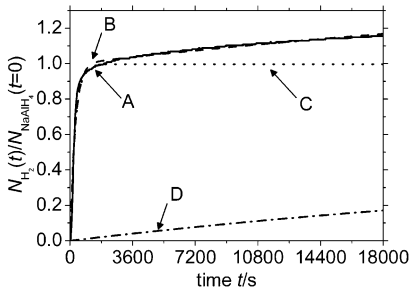

Figure 1. Dehydrogenation of Ti-doped $NaAlH_4$ at 423 K. (A) Experimental. (B) Theoretical: total (eq 10). (C) Theoretical: contribution from the dehydrogenation of $NaAlH_4$ (first term on the right side of eq 10). (D) Theoretical: contribution from Na_3AlH_6 (second term on the right side of eq 10).

$$k_i = \kappa\frac{k_B T}{h}\exp\left(-\frac{\Delta G^{\ddagger}}{RT}\right) \tag{11}$$

where κ is the transmission coeffcient, k_B is the Boltzmann constant, h is Planck's constant, T is the absolute temperature, and R is the gas constant. Assuming that κ is independent of the temperature, substituting $\Delta G^{\ddagger} = \Delta H^{\ddagger} - T\Delta S^{\ddagger}$, where $\Delta H^{\ddagger}$ and $\Delta S^{\ddagger}$ are respectively the enthalpy and entropy of activation, into eq 11 and rearranging and taking the logarithm gives

$$\ln\left(\frac{k_i}{T}\right) = -\frac{\Delta H^{\ddagger}}{R}\frac{1}{T} + \text{constant} \tag{12}$$

Results and Discussion

The overall dehydrogenation profile of $NaAlH_4$ doped with 2 mol % $Ti(OBu^n)_4$ (Ti-doped $NaAlH_4$) is seen in Figure 1, The solid line represents the hydrogen evolution $N_{H_2}(t)$ from Ti-doped $NaAlH_4$ at 423 K. The profile is composed of two portions: a rapid reaction ($0 \le t/s \le 1000$) followed by a slow reaction ($1000 \le t/s$). Obviously, the first reaction corresponds to the dehydrogenation of $NaAlH_4$ (eq 1) and the second to the dehydrogenation of Na_3AlH_6 (eq 2). The broken line in the figure shows the close simulation of the profile that was obtained by using eq 10 and values of $k_1 = 3.5 \times 10^{-3}\ s^{-1}$ and $k_2 = 2.3 \times 10^{-5}\ s^{-1}$. These rate constants confirm earlier observations that the first dehydrogenation reaction in the stepwise dehydrogenation of Ti-doped $NaAlH_4$ is much faster than the second.[5,7,11,15,20,22] In the case of $NaAlH_4$ doped with 2 mol % $Zr(OPr^n)_4$ (Zr-doped $NaAlH_4$), the second step is so much slower than the first one that the rate constant, k_2, could not be determined within a practical time frame. A priori, these results suggest that both the titanium and zirconium dopants provide a much more pronounced intrinsic kinetic enhancement to the first dehydrogenation reaction. However, further experiments, described below, have shown that this is not the case. Although the experimental profile is closely simulated by eq 10 at 423 K, it deviates significantly from the model at temperatures lower than 383 K. This is apparently due to kinetic complications imposed processes not considered in eq 10 (i.e., nucleation and growth or atomic diffusion) that are likely to limit this solid state transformation at the lower temperatures. To clarify the kinetic constraints on the dehydrogenation process, we decided to determine the rate constants k_1 and k_2 of eqs 1 and 2 individually through independent measurement of the dehydrogenation kinetics of the Ti- and Zr-doped $NaAlH_4$ and Na_3AlH_6.

Na_3AlH_6 was prepared through dehydrogenation of $NaAlH_4$ in a 350 mL stainless steel reactor at 480−490 K for 3 h

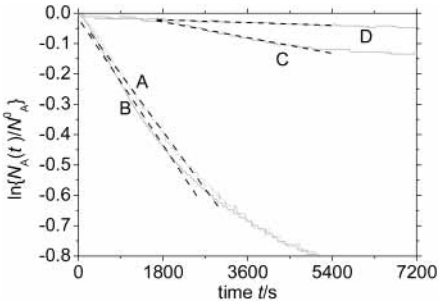

Figure 2. Comparison of the dehydrogenation profiles at 383 K of (A) Ti-doped $NaAlH_4$; (B) Ti-doped Na_3AlH_6; (C) Zr-doped $NaAlH_4$; and (D) Zr-doped Na_3AlH_6.

TABLE 1: Dehydrogenation Rate Constants (k/s^{-1}) of Ti- and Zr-Doped $NaAlH_4$ and Na_3AlH_6

	Ti-doped		Zr-doped	
T/K	$NaAlH_4$	Na_3AlH_6	$NaAlH_4$	Na_3AlH_6
363	2.3×10^{-5}[a]		1.3×10^{-6}	
373	2.0×10^{-4}[a]	7.7×10^{-5}	6.6×10^{-6}	
383	2.4×10^{-4}[a]	2.6×10^{-4}	3.2×10^{-5}	4.5×10^{-6}
393	4.8×10^{-4}	5.0×10^{-4}[a]	8.6×10^{-5}	1.4×10^{-6}[a]
403	1.1×10^{-3}[a]	1.1×10^{-3}	2.1×10^{-4}	2.9×10^{-5}[a]
413	2.4×10^{-3}[a]	2.6×10^{-3}[a]	4.7×10^{-4}	1.1×10^{-4}[a]
423	4.8×10^{-3}	3.6×10^{-3}	8.7×10^{-4}	2.8×10^{-4}[a]

[a] Average of two determinations.

according to the procedure of Ashby.[25] Analysis of the product by X-ray diffraction confirmed it to be a mixture of Na_3AlH_6 and Al with no traces of $NaAlH_4$. Measurement of the amount of hydrogen released during heating also verified that the reaction seen in eq 1 proceeds to completion.

Figure 2 compares the dehydrogenation profiles of Ti- and Zr-doped $NaAlH_4$ with those of Ti- and Zr-doped Na_3AlH_6 at $T = 383$ K. Determination of the slopes of the dehydrogenation profiles (indicated by the broken lines in Figure 2) during the acceleratory period gives the rate constants[26] k_1 and k_2 in terms of eq 4: $k_1 = 2.4 \times 10^{-4}$ s^{-1} and $k_2 = 2.6 \times 10^{-4}$ s^{-1} for Ti-doped hydrides; and $k_1 = 3.2 \times 10^{-5}$ s^{-1} and $k_2 = 4.5 \times 10^{-6}$ s^{-1} for Zr-doped hydrides. Thus the dehydrogenation of Na_3AlH_6 that is directly doped with Ti or Zr undergoes dehydrogenation at much faster rates than those observed for the hexahydride arising from the dehydrogenation of doped $NaAlH_4$. Remarkably, the rates observed for directly Ti-doped Na_3AlH_6 *match* those of Ti-doped $NaAlH_4$. However, hexahydride that is directly doped with Zr undergoes significantly slower dehydrogenation than Zr-doped $NaAlH_4$.

Kinetic measurements were carried out over temperature ranges of 363−423 K for Ti- and Zr-doped $NaAlH_4$, 373−423 K for Ti-doped Na_3AlH_6, and 383−423 K for Zr-doped Na_3AlH_6. To check the reproducibility and the reliability of the data, the measurements were repeated twice for some temperatures using different batches of hydride. The dehydrogenation rates of Ti-doped $NaAlH_4$ and Na_3AlH_6 were consistently found to be much higher than those of the Zr-doped hydrides. The obtained rate constants are summarized in Table 1. The activation enthalpies, $\Delta H^{\ddagger}$, of dehydrogenation were determined from the Eyring plots ($\ln(k/T)$ vs $1/T$) shown in Figure 3. The values derived for $\Delta H^{\ddagger}$ are summarized in Table 2. Although the standard deviations are large, it can be concluded that the activation enthalpies of dehydrogenation of Ti-doped $NaAlH_4$ and Na_3AlH_6 are lower than those of the Zr-doped hydrides. For both the Ti- and Zr-doped hydrides, the activation enthalpies of $NaAlH_4$ and Na_3AlH_6 are comparable: i.e., $\Delta H^{\ddagger}$ (Ti-doped $NaAlH_4$) $\approx$ $\Delta H^{\ddagger}$ (Ti doped Na_3AlH_6) $\approx$ 100 kJ·mol^{-1} and $\Delta H^{\ddagger}$ (Zr-doped $NaAlH_4$) $\approx$ $\Delta H^{\ddagger}$ (Zr doped Na_3AlH_6) $\approx$ 135 kJ·mol^{-1}.

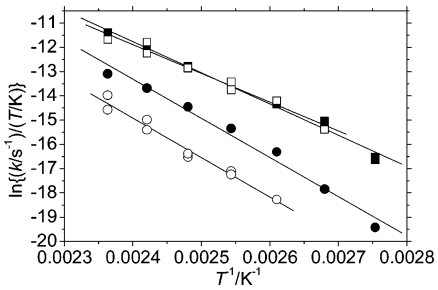

Figure 3. Eyring plots of rate constants for the dehydrogenation of (A) Ti-doped $NaAlH_4$ ■; (B) Ti-doped Na_3AlH_6 □; (C) Zr-doped $NaAlH_4$ ●; and (D) Zr-doped Na_3AlH_6 ○.

TABLE 2: Enthalpies of Activation, $\Delta H^{\ddagger}$, of Ti- and Zr-Doped $NaAlH_4$ and Na_3AlH_6 (in kJ per mol)

	Ti-doped	Zr-doped
$NaAlH_4$	100 ± 7	134 ± 16
Na_3AlH_6	99 ± 13	135 ± 17

Conclusions

We have observed that both $NaAlH_4$ and Na_3AlH_6 undergo dehydrogenation at nearly equal rates directly following mechanical doping with titanium. This finding was quite unexpected, as the Na_3AlH_6 arising from the initial dehydrogenation of Ti-doped $NaAlH_4$ undergoes dehydrogenation at much slower rates. Thus Ti doping does not innately enhance the dehydrogenation $NaAlH_4$ to a greater extent than Na_3AlH_6. Instead it seems plausible that the dehydrogenation of doped $NaAlH_4$ yields Na_3AlH_6 in which the Ti dopant is not properly distributed for the maximum enhancement of the dehydrogenation of the hexahydride. Our finding that Ti-doped $NaAlH_4$ and Na_3AlH_6 undergo dehydrogenation at the same rates clearly indicates that the dehydrogenation kinetics are insensitive to variation in the Al−H bonding interactions and are probably influenced by processes such as nucleation and growth or the diffusion of atoms and molecules. These processes may be less important in determining the dehydrogenation kinetics of Zr-doped $NaAlH_4$ and Na_3AlH_6, as, unlike the Ti-doped materials, directly Zr-doped Na_3AlH_6 undergoes dehydrogenation at significantly different rates than Zr-doped $NaAlH_4$.

At high temperatures (ca. 423 K) the two-step dehydrogenation of Ti-doped $NaAlH_4$ to NaH is well represented by a consecutive, first-order reaction kinetics given by eq 7. However, at temperatures lower than 383 K, the dehydrogenation kinetics deviate significantly from this model. This observation provides further confirmation that processes other than the breaking of Al−H bonds in the complex anions play significant roles in determining the rates of dehydrogenation of these materials at lower temperatures.

We have found excellent agreement in the values determined for the activation enthalpies of the dehydrogenation of $NaAlH_4$ and Na_3AlH_6 with the same dopant (Ti doped $\approx$ 100 kJ per mol and Zr doped $\approx$ 135 kJ per mol). This suggests that the dehydrogenation mechanisms of Ti- and Zr-doped $NaAlH_4$ and Na_3AlH_6 all involve similar reaction pathways in which the dominant energetic consideration is the positioning of dopants rather than the strength of Al−H bonding interactions. In situ X-ray diffraction[8] and scanning electron microscopy[17] studies have shown that the phases arising from the dehydrogenation of Ti-doped $NaAlH_4$ are composed of large crystallites with

sizes greater than 100 nm. These findings indicate that processes must be operating in which the constituent metal atoms are transported over a long range. Interestingly, the values of $\Delta H^{\ddagger}$ that we have determined in this study are close to the value reported for the self-diffusion activation energy of metallic aluminum of 142 kJ·mol^{-1}.[27] This suggests that the rate-determining step in the dehydrogenation of the doped alanates at lower temperatures may also be a long-range atomic transport phenomenon.

Studies currently in progress of the rehydrogenation kinetics should reinforce our conclusions and perhaps provide further insight. Additionally, microscopic studies of the dehydrogenation reactions based on the knowledge obtained from our macroscopic observations should elucidate the details of the reaction mechanism(s) and function of dopants.

Acknowledgment. The study was administered through the New Energy and Industrial Technology Development Organization (NEDO) as a part of the International Clean Energy Network using Hydrogen Conversion (WE-NET) program with funding from the Ministry of Economy, Trade and Industry of Japan.

References and Notes

(1) Gravimetric hydrogen density targets of 5.0, 6.0, and 5 wt % have been set by the Japanese government, WE-NET project (http://www.enaa.or.jp/WE-NET), the International Energy Agency (http://hydpark-.ca.sandia.gov/iea.html), and the U.S. Department of Energy (http://www.eere.energy.gov/hydrogenandfuelcells/mission), respectively.

(2) Bowman, R. C.; Fultz, B. *MRS Bull.* **2002**, *27*, 688.

(3) Bogdanovic, B.; Schwickardi, M. *J. Alloys Compd.* **1997**, *253*−*254*, 1.

(4) Bogdanovic, B.; Schwickardi, M. International Patent WO97/03919, 1997.

(5) Jensen, C. M.; Zidan, R.; Mariels, N.; Hee, A. G.; Hagen, C. *Int. J. Hydrogen Energy* **1999**, *23*, 461.

(6) Zidan, R. A.; Takara, S.; Hee, A. G.; Jensen, C. M. *J. Alloys Compd.* **1999**, *285*, 119.

(7) Bogdanovic, B.; Brand, R. A.; Marjanovic, A.; Schwickardi, M.; Tölle, J. *J. Alloys Compd.* **2000**, *302*, 36−58.

(8) Gross, K. J.; Guthrie, S.; Takara, S.; Thomas, G. *J. Alloys Compd.* **2000**, *297*, 270.

(9) Zaluska, A.; Zaluski, L.; Ström-Olsen, J. O. *J. Alloys Compd.* **2000**, *298*, 125.

(10) Balema, V. P.; Dennis, K. W.; Pecharsky, V. K. *Chem. Commun.* **2000**, 1665.

(11) Jensen, C. M.; Gross, K. J. *Appl. Phys. A* **2001**, *72*, 213.

(12) Bogdanovic, B.; Schwickardi, M. *Appl. Phys. A* **2001**, *72*, 221.

(13) Chen, J.; Kuriyama, N.; Xu, Q.; Takeshita, H. T.; Sakai, T. *J. Phys. Chem. B* **2001**, *105*, 11214.

(14) Jensen, C. M.; Zidan, R. A. U.S. Patent 6,471,935, 2002.

(15) Gross, K. J.; Thomas, G. T.; Jensen, C. M. *J. Alloys Compd.* **2002**, *330*−*332*, 691.

(16) Gross, K.; Sandrock, G.; Thomas, G.; Jensen, C.; Meeker, D.; Takara, S. *J. Alloys Compd.* **2002**, *330*−*332*, 696.

(17) Thomas, G. J.; Gross, K.; Yang, N. Y. C.; Jensen, C. M. *J. Alloys Compd.* **2002**, *330*−*332*, 702.

(18) Sun, D.; Kiyobayashi, T.; Takeshita, H. T.; Kuriyama, N.; Jensen, C. M. *J. Alloys Compd.* **2002**, *337*, L8.

(19) Meisner, G. P.; Tibbetts, G. G.; Pinkerton, F. E.; Olk, C. H.; Balogh, M. P *J. Alloys Compd.* **2002**, *337*, 254.

(20) Sandrock, G.; Gross, K.; Thomas, G. *J. Alloys Compd.* **2002**, *339*, 299.

(21) Fichtner, M.; Fuhr, O. *J. Alloys Compd.* **2002**, *345*, 286.

(22) Bogdanovic, B.; Sandrock, G. *MRS Bull.* **2002**, *27*, 712.

(23) Balogh, M. P.; Tibbetts, G. G.; Pinkerton, F. E.; Meisner, G. P.; Olk, C. H. *J. Alloys Compd.* **2003**, *350*, 136.

(24) Glasstone, S.; Laidler, K. J.; Eyring, H. *The Theory of Rate Processes*; McGraw-Hill: New York, 1941; p 11.

(25) Ashby, E. C.; Kobertz, P. *Inorg. Chem.* **1966**, *5*, 1615.

(26) Young, D. A. *The International Encyclopedia of Physical Chemistry and Chemical Physics Topic 21: Solid and Surface Kinetics Vol 1: Dehydrogenation of Solids*; Pergamon Press: Oxford, 1966.

(27) Borg, R. J.; Dienes, G. J. *The Physical Chemistry of Solids*; Academic Press: San Diego, 1992; p 466.